# MMTO Conversion Technical Memorandum #00-2


Smithsonian Institution &
The University of Arizona®

## Correcting 6.5m Primary Mirror Figure Errors with the Active Supports

**S. C. West, H. M. Martin**

**January 18, 2000**

# Correcting 6.5m Primary Mirror Figure Errors with the Active Supports

*MMT Conversion Technical Memo #00-2, 18 Jan 2000*

S. C. West
Multiple Mirror Telescope Observatory, Tucson, AZ

and H. M. Martin
Steward Observatory Mirror Lab, Tucson, AZ

*Abstract*

*We summarize the procedure required to produce an axial force distribution that corrects primary mirror figure errors observed at the telescope. The relationship of the wavefront observables to the mirror bending influence functions is shown. Results from mode-filtering the solution in order to control large cancelling forces of neighboring actuators are briefly investigated. URLs are given for matrices that convert wavefront phase errors to the compensating axial force distribution allowing data from other wavefront-measuring instruments to be used.*

## I. Intro

BCV progetti has calculated the x, y, and z surface distortions resulting from force applied to the mirror blank by each of 52 axial actuators[1]-[4]. By using the active support system, these axial influence functions have been used successfully to correct figure distortions of the MMT and Magellan primary mirrors in laboratory conditions[5].

This memo summarizes the calculations appropriate for converting wavefront errors observed at the telescope into the compensating set of axial correction forces. It provides computational detail helpful to others wishing to correct mirror figure distortion with their own instrumentation.

Section III has a description and location of the data files used for correcting mirror figure with the active support system.

## II. Calculations

### *A. Surface distortion influence functions*

BCV has provided theoretical x,y,z mirror surface displacements at 3222 nodes resulting from the application of force from each of 52 axial actuators (Figure 1). These vectors represent the displacement of the distorted surface from the ideal surface. The node distortions for the remaining 52 actuators are obtained by applying symmetry rules. So we have a set of surface distortion influence functions for each of the 104 axial actuators:

$$\frac{\partial(x, y, z)_i}{\partial F_j} \tag{1}$$

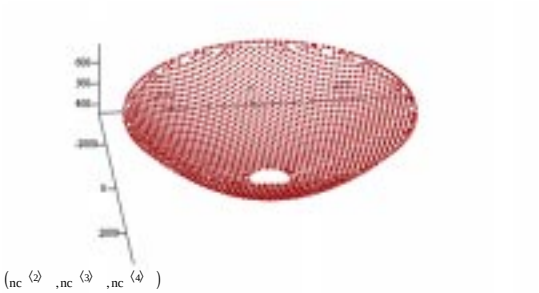

Figure 1: Distribution of nodes where the surface distortions are tabulated by BCV progetti.

where “i” is the node number and “j” is the actuator number.

### *B. Wavefront influence functions*

In practice, the surface displacement influence functions themselves are not directly observed by the instrumentation. For example, observations taken in the laboratory at the vertex radius of curvature are sensitive to twice the surface normal component of the BCV displacement vector.

The pathlength error sensed by an instrument attached to the telescope is shown in Figure 2. The wavefront pathlength error created by the displaced surface is d1+d2. $N_z$ is the z-component of the displacement normal to the ideal (undistorted) surface. After applying the law of sines, and the half-angle trigonometric identity, we find:

$$Nz_i = \frac{1}{2}(d1_i + d2_i) \tag{2}$$

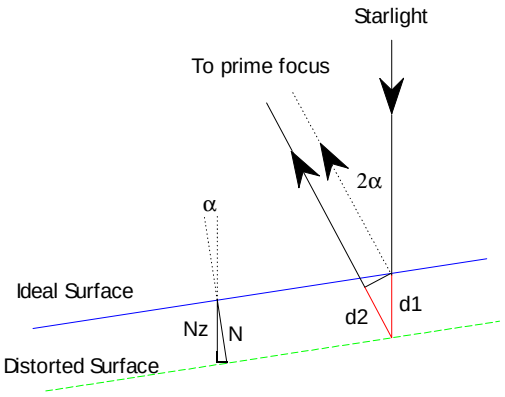


Figure 2: Exaggerated pathlength error of starlight reflecting from a distorted primary mirror at node i.

In other words, the wavefront phase error $\Delta w_i$ observed at node "i" is twice the z-component of the distortion normal to the surface at that point $2Nz_i$ (this is different than d1 which is the z-component of the total surface distortion at "i"). Thanks to Giancarlo Parodi for pointing this out.

### *C. Axial correction forces*

From Equation 2, the axial force distribution and the wavefront distortion it produces are related by:

$$\begin{bmatrix} \frac{\partial w_1}{\partial F_1} & \cdots & \frac{\partial w_1}{\partial F_N} \\ \cdots & & \cdots \\ \frac{\partial w_M}{\partial F_1} & \cdots & \frac{\partial w_M}{\partial F_N} \end{bmatrix} \begin{bmatrix} F_1 \\ \cdots \\ F_N \end{bmatrix} = \begin{bmatrix} \Delta w_1 \\ \cdots \\ \Delta w_M \end{bmatrix} \quad (3)$$

The columns of the matrix $\partial w_i / \partial F_j$ express the effect of each axial support actuator upon the wavefront. These wavefront influence functions are obtained by transforming the BCV *surface deflection* influence functions that are described in Section IIa. Each BCV data file expresses the vector displacement of the distorted surface from the ideal surface for 3222 points on the mirror surface. To convert these surface displacements into wavefront distortions:

- Project the BCV displacement vector onto the direction normal to the surface to obtain the normal displacement vector N.
- Take twice the z-component of N.
- Remove the global tilts and piston from the result.

The wavefront influence matrix can be inverted with singular value decomposition (SVD) allowing the axial correction forces $(F)$ to be determined from a measured *wavefront* distortion $(\Delta w)$.

In practice, any wavefront sensor (*e.g.*, slope sensor, curvature sensor, shearing interferometer, phase sensor) may be used along with a corresponding set of influence functions. Our current algorithm finds the wavefront distortions at the BCV nodes $(\Delta w)$ by re-sampling Zernike polynomials determined with an interferometric Hartmann sensor.

### *D. High-order mode filtering*

The SVD solution allows the removal of modes which do not contribute to the solution. This is accomplished by selectively nulling terms in the diagonal matrix per standard rules. After removing these few terms, we still find that the resulting actuator force distribution contains spurious groupings of large cancelling forces from neighboring actuators. Simulations were run comparing the P-P actuator forces of the correction with the resulting improvement in surface quality. Three simulations are shown in Tables 1-3.

Table 1: filtering of force solution from a mirror lab error surface

| Retained Modes | rms of final surface nm | p-p actuator forces N |
|---|---|---|
| 101 | 21 | 640 |
| 36 | 23 | 231 |
| 32 | 23 | 230 |
| 27 | 26 | 181 |
| 0 | 36 | 0 |

Table 2: filtering of force solution for a Z4 = 400nm error surface

| Retained Modes | rms of final surface nm | p-p actuator forces N |
|---|---|---|
| 101 | 1.0 | 57 |
| 36 | 1.8 | 26 |
| 32 | 1.8 | 26 |
| 27 | 2 | 23 |
| 0 | 172 | 0 |

Table 3: filtering of force solution for Z4 = 200nm, Z6 = 200nm error surface

| Retained Modes | rms of final surface nm | p-p actuator forces N |
|---|---|---|
| 101 | 10 | 390 |
| 36 | 12 | 106 |
| 32 | 14 | 82 |
| 27 | 15 | 71 |
| 0 | 115 | 0 |

Each table shows the number of lowest-order solution modes retained (0 means no correction of the distorted surface, 101 means all modes except the two which don't contribute to the solution). Also shown is the rms figure error remaining after application of the correcting forces, and the peak-to-peak actuator force difference of the correction. Table 1 shows a

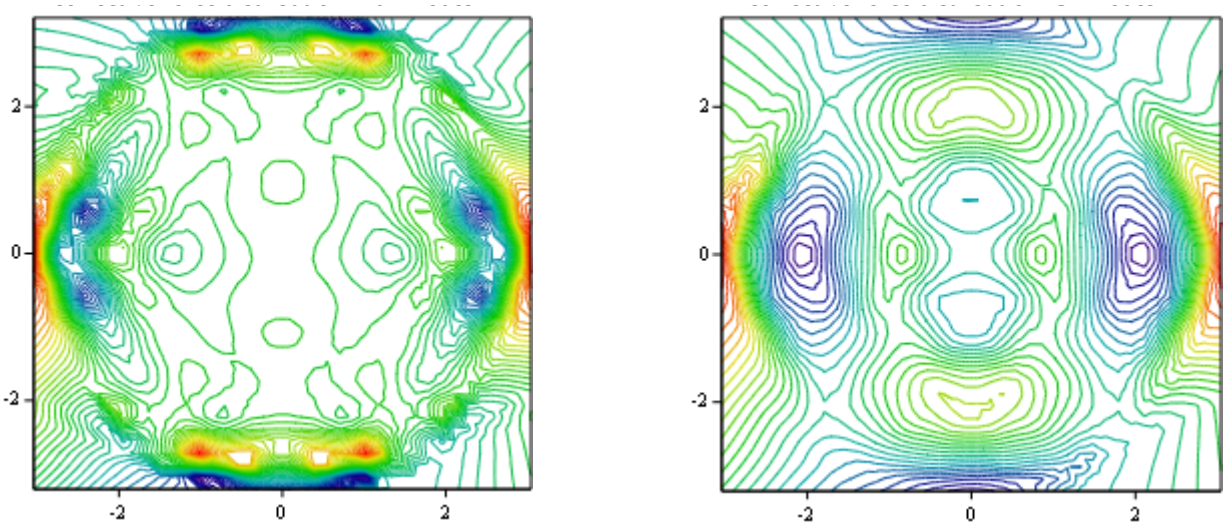


Figure 3: Contours of the corrective force distribution that compensates a surface astigmatism figure error without (left for 101 modes) and with (32 modes) filtering of the solution. The graphs correspond to two of the cases shown in Table 2. Spurious contours are shown outside of the mirror diameter.

simulation starting with a real mirror distortion observed in the mirror lab, table 2 for pure Zernike astigmatism and table 3 for an astigmatism/coma mixture.

In all cases, filtering produces a dramatic reduction in the spread of spurious actuator forces with relatively little penalty in residual figure error. The force distribution that corrects surface astigmatism is shown in Figure 3 with and without smoothing of the solution.

## III. Data files

This section provides URLs to various data files that can be used to correct figure distortion. The matrices are applicable only to the geometry described in section II B (*i.e.*, not to radius of curvature testing).

All of the following files can be found in the directory: http://nemo.as.arizona.edu/~swest/figureCorrection/

- figureCorrectionsMemo.pdf, ps: This memo in pdf and PS formats.
- Surf2ActTEL_104.bin: 3222 x 104 matrix stored in binary format. When multiplied by a *surface* phase error vector (nm) arranged in the order of the bcv nodes, it outputs 104 axial actuator forces (N) that correct the distortion.
- Surf2ActTEL_32.bin: same as 104.bin except only the lowest 32 modes are retained in the solution. This is currently the matrix used at the MMT for correcting figure distortion.
- Act2SurfTEL: outputs surface node phases for a given actuator force distribution (matrix is stored as text).
- bcv.c: This is a self-documented c-program that performs the calculations outlined in this memo. It's not a stand-alone program -- it's part of the suite of programs for the MMT interferometric Hartmann wavefront sensor that are controlled with a TCL/TK GUI running under linux -- but it illustrates how to read the binary matrices, resample the Zernike polynomials, and perform the matrix arithmetic.
- nodecoor: BCV node coordinates (mm) used for resampling the Zernike surface.
- We also have several MathCad files available that perform all the calculations: BCV_influenceTel.pdf, bcv_linked list.pdf, zernikeBCVnodes.pdf, and Forc_corr.pdf.

## IV. References

[1] BCV progetti, "MMT Conversion Project: *MMT 6.5m F/1.25: Axial Supports Influence Functions*," **Report #8 Rev. 0**, 1995 January, Milano.

[2] BCV progetti, "MMT Conversion Project: *Mirror 6.5m F/1.25: Axial and Lateral Support Optimisation*," **Report #7 Rev. 0**, 1994 December, Milano.

[3] BCV progetti, "MMT Conversion Project: *Mirror 6.5m F/1.25: Finite Element Model*," **Report #6 Rev. 0**, 1994 November, Milano.

[4] BCV progetti, Columbus Project: A proposal for a new set of functions fitting surface defects," Columbus **Report #143 Rev. 0**, 1992 March, Milano.

[5] H.M. Martin, S.P. Callahan, B. Cuerden, W.B. Davison, S.T. DeRigne, L.R. Dettmann, G. Parodi, T.J. Trebisky, S.C. West, and J.T. Williams, "*Active Supports and Force Optimization for the MMT Primary Mirror*," Advanced Technology Optical Telescopes VI, L.M. Stepp ed., SPIE **3352**, 513 (1998).